Available online at http://ijcpe.uobaghdad.edu.iq and www.iasj.net
Iraqi Journal of Chemical and Petroleum Engineering
Vol.20 No.2 (June 2019) 23 – 32
EISSN: 2618-0707, PISSN: 1997-4884

Adsorption of Chromium Ions on Activated Carbon Produced from Cow Bones

Marah Waleed Khalid and Sami D. Salman

Alkhwarizmi College of Engineering, University of Baghdad, Baghdad, Iraq

Abstract

Due to the broad range uses of chromium for industrial purposes, besides its carcinogenic effect, an efficient, cost effective removal method should be obtained. In this study, cow bones as a cheap raw material were utilized to produce active carbon (CBAC) by physiochemical activation, which was characterized using: SEM to investigate surface morphology and BET to estimate the specific surface area. The best surface area of CBAC was 595.9 m^2/gm which was prepared at 600 $^{\circ}$C activation temperature and impregnation ratio of 1:1.5. CBAC was used in aqueous chromium ions adsorption. The investigated factors and their ranges are: initial concentration (10-50 mg/L), adsorption time (30-300 min), temperature (20-50 $^{\circ}$C) and solution pH (2-11). Isotherm of adsorption and its kinetics were studied. The adsorption process was modeled statistically and was represented by an empirical model. Equilibrium data were fitted to the Langmuir and Freundlich isotherm models and the data best represented by Freundlich isotherm. Pseudo- first order and pseudo- second order kinetic equations were utilized to study adsorption kinetics, where chromium adsorption on CBAC fitted pseudo- second order fitted the data more adequately. The best removal efficiency was found to be 94.32%.

Keywords: Adsorption, activated carbon, cow bones, chromium, physiochemical activation.

Received on 06/02/2019, Accepted on 23/03/2019, published on 30/06/2019

https://doi.org/10.31699/IJCPE.2019.2.4

1- Introduction

Due to the wide range and the exaggerated uses of organic solvents, oxidizing agents, phenols and heavy metals in industry, they were accumulated in the environment, which led some ecosystems to deteriorate.

Heavy metals category is one of the most harmful pollutants of surface and ground waters. Industrial effluents are the primary source. Because almost all of the heavy metals could not be degraded to harmless components [1]; therefore reduction of heavy metals concentrations before discharging them into rivers had become a necessity. Otherwise, they could be harmful to health and/or reduce drinking water quality [2].

According to the World Health Organization (WHO, 1984) and International Program on Chemical Safety (IPCS, 1988), the most toxic metals are aluminum, zinc, mercury, arsenic, chromium, nickel, copper, cadmium and lead. The drinking water guideline value recommended by the World Health Organization (WHO) and Iraqi standard regulation is 0.01 and 0.015 mg Pb/l.

Chromium is found in freshwaters due to its extensive use in petrochemical, electronics, tanneries, electroplating industries, mining operations, as well as in textile mill products [3]. Chromium is carcinogenic [4] and causes severe damage to human organs: e.g., to the kidneys, the brain, reproductive system, the liver, and the nervous system [5].

As a result of the toxicity of this element and its compounds, removal has become an urgent priority. There are various available means to reduce heavy metals levels from water including ion exchange [6], [7], membrane filtration [8], [9], chemical precipitation [10], [11] and electrocoagulation [12], [13], but these methods generally require high cost and produce more lethal products [14].

Adsorption on solid materials is one of the best existing methods for the refinement of water and the regulation of atmospheric and aquatic pollution, with active carbon being the most used adsorbent in the industry [6]. In the last years, global consumption of active carbon has increased by an average annual increase of 5.5% and it is anticipated to continue to do so at a higher rate in next years (8.1% in 2018)[15].

Activated carbon has been established as effective adsorbents for the removal of a wide variety of pollutants dissolved in aqueous media, or from the gaseous environment due to its exceptionally high surface areas, well-developed internal micro porosity structure as well as the presence of a broad spectrum of surface functional groups [16].

Thus, locally produced wastes such as cow bones, saw dust and others were examined for preparing active carbon. Because of the low cost of those wastes, a high percentage of carbonaceous contents and their abundance they were utilized to produce cost effective, efficient activated carbon and applicate it to remove heavy metals.

Corresponding Authors: Name: Marah Waleed Khalid , Email: mw.alsharod@gmail.com, Name: Sami D. Salman, Email: sami.albayati@gmail.com

2- Materials And Methods

2.1. Adsorbate

Technical grade Potassium dichromate ($K_2Cr_2O_7$) of 99.8% purity provided by Himedia, Germany was used to preparing the stock solution of chromium. All solutions were prepared using distilled water.

The stock of 1000 mg/L was prepared by adding (2.8269) gm of $K_2Cr_2O_7$ to a liter of DW; dilution law was used to prepare the required concentrations. 0.1 M HNO_3 and 0.1 M NaOH were used to adjust the pH [17]

2.2 Chemicals and Gases

Name	Formula	Assay (%)	Source or company	Usage
Nitrogen	N_2	99.9	local	Inert gas to prevent raw material combustion
Potassium Hydroxide pellet	KOH	85	Himedia, India	Chemical activating agent
Carbon dioxide	CO_2	99.9	local	Physical activating agent
Hydrochloric acid	HCl	2N	England	Washing and Neutralizing of AC
Potassium dichromate	$K_2Cr_2O_7$	99.9	Thomas Baker, India	Chromium ions source
Nitric acid	HNO_3	70	J.T.Baker, Holland	solution pH adjustment
Sodium hydroxide	NaOH	99.5	DIDACTIC, Spain	solution pH adjustment

2.3. Preparation and Characterization of Activated Carbon

Cow bones (CB) was collected from local butchers, Baghdad, Iraq as waste. The preparation methodology of CBAC is concise in Fig. **1**.

The conditions that were used in cow bone charring were obtained from Moreno-piraján [18].

The surface area was analyzed using Brunaure-Emmett-Teller (BET: HORIBA, SA-900 series, USA) through nitrogen adsorption isotherm at 77 K.

In order to determine the shape of the CBAC surface, the samples were scanned using a Scanning Electron Microscope (TESCAN, Vega III, Czech Republic).

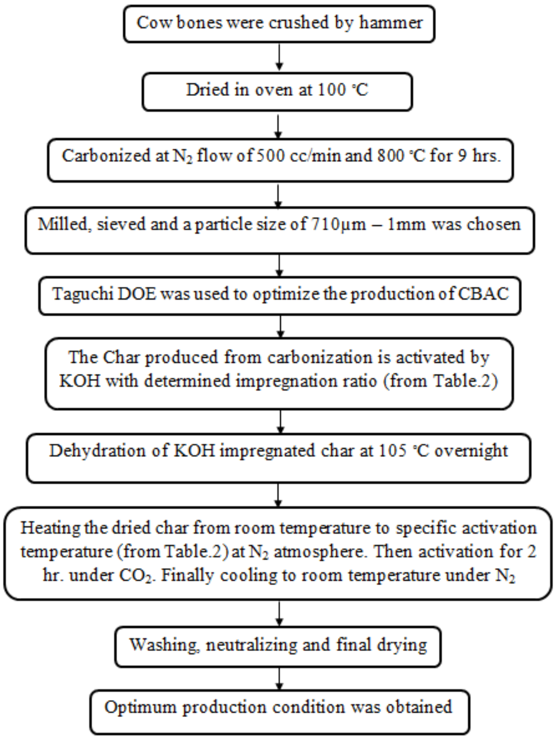

Fig. 1. Schematic diagram for the CBAC preparation steps

2.4. Design of Experiments

The experimental design usually used to efficiently map the set of experiments to be conducted and to serve the following:

- understand the effect of the factors and/or
- model the relationship between response and factors

with a minimum of experiments [19].

Taguchi method was used in the optimization of the CBAC production and modeling of adsorption process due to its efficiency compared to other methodologies and its robustness. STATISTICA 10 (StatSoft, Inc. USA) was used to design the set of experiments**.** Table **1** shows the L9 orthogonal array that was chosen (2 factors, 3 levels) for CBAC preparation and Table **2** shows the L25 array (4 factors, 4 levels) for chromium adsorption process.

Table 1. Taguchi DOE (L9 array) of CBAC optimization

No.	Activation temperature (°C)	IR
1	600	1:0.5
2	600	1:1
3	600	1:1.5
4	700	1:0.5
5	700	1:1
6	700	1:1.5
7	800	1:0.5
8	800	1:1
9	800	1:1.5

Table 2. Taguchi DOE (L25 array) of Chromium adsorption experiments

No.	Initial concentration (mg/L)	Contact time (minutes)	Temperature (C^o)	Solution pH
1	10	30	20	2
2	10	120	30	5
3	10	210	40	8
4	10	300	50	11
5	20	30	30	8
6	20	120	20	11
7	20	210	50	2
8	20	300	40	5
9	30	30	40	11
10	30	120	50	8
11	30	210	20	5
12	30	300	30	2
13	50	30	50	5
14	50	120	40	2
15	50	210	30	11
16	50	300	20	8

2.5. Batch Equilibrium Studies

Bach mode adsorption experiments were conducted by adding a specific amount of adsorbent to a 100 ml chromium solution contained in a 100 ml capped plastic containers. The containers were placed in an isothermal shaker (JSSI-300CL, JSR, Korea) at an agitation speed of 180 rpm. The remaining concentration of chromium in each sample after adsorption at different times was determined by atomic-absorption spectroscopy (Shimadzu AA6200, Japan). All samples were filtered from the adsorbent with Whatmen filter paper to make it carbon free. The chromium concentration adsorbed on CBAC was predicted according to:

$$q_e = \frac{(C_o - C_e)V}{W} \qquad (1)$$

Where q_e is the adsorption capacity at equilibrium (mg/g), C_o and C_e are the concentrations at initial and equilibrium conditions (mg/L) for chromium solution, respectively; V is the volume (L); and W is the weight (g) of CBAC.

2.6. Adsorption Process Modelling

After adsorption batch experiments were run, the equilibrium concentrations (C_e) were used to form a mathematical model that represents the adsorption process.

This model relates C_e as a response with the investigated factors which are: initial concentration, contact time, temperature, and solution pH. STATISTICA 10 (StatSoft, Inc. USA) was utilized to form the model by nonlinear estimation method.

This model was used to generate the equilibrium concentration at various conditions; these results were used in adsorption isotherm fitting, kinetics study, and adsorption thermodynamics.

2.7. Adsorption Isotherm

Two isotherm models (Langmuir and Freundlich) were used to fit the equilibrium data. The linear form of the Langmuir [20] model is:

$$\frac{1}{q_e} = \frac{1}{q_m} + \frac{1}{(k_a q_m)}\frac{1}{C_e} \qquad (2)$$

Where C_e (mg/l) is the concentration of chromium at equilibrium; q_e (mg/g) the equilibrium adsorption capacity; q_m the adsorption capacity for a complete monolayer (mg/g); K_a (L/mg) is the constant of adsorption equilibrium. The linear form of Freundlich [21] isotherm is:

$$\ln q_e = \ln K_F + \left(\frac{1}{n}\right)\ln C_e \qquad (3)$$

The constants K_F (mg/g) and n are the Freundlich constants.

2.8. Kinetic Studies

The adsorption rate constants were predicted from the pseudo-first-order and pseudo-second-order equations. For the pseudo-first-order, the Lagergren [22] the used expression is:

$$\log(q_e - q_t) = \log q_e - \frac{k_1 t}{2.303} \qquad (4)$$

Where q_e and q_t (mg/g) are the adsorption capacities equilibrium and at time t (min), respectively and k_1 (1/min) is the adsorption constant. The linear form of the pseudo-second-order [23] reaction can give by:

$$\frac{t}{q_t} = \frac{1}{k_2 q_e^2} + \frac{1}{q_e}t \qquad (5)$$

Where the adsorption capacity of equilibrium (q_e), and the constant of second order k_2 (g/mg h) can be determined experimentally from the intercept and slope of t/qt versus t plot.

3- Results and Discussion

3.1. CBAC Production and Optimization

The complete design array (L 9) for the surface area and yield as responses of CBAC preparation with two factors, temperature of activation and impregnation ratio (IR)(char: KOH wt: wt) from the experiments that were conducted are shown in Table **3**.

Table 3. Preparation of CBAC experimental design array and the results for SSA and yield

Runs	CBAC preparation variables		CBAC preparation responses	
	IR	Activation temperature (°C)	Specific surface area (m^2/gm)	Yield (%)
1	1:0.5	600	270.4	85.9
2	1:0.5	700	475.6	79.3
3	1:0.5	800	370.4	71.4
4	1:1	600	315.3	79.5
5	1:1	700	480.6	72.2
6	1:1	800	460.0	60.6
7	1:1.5	600	595.9	76.2
8	1:1.5	700	350.0	65.3
9	1:1.5	800	240.8	57.9

It was found that in CBAC preparation the SSA increases as IR rises from 1:0.5 to 1:1. These results clarify that the reduction of KOH occurs during the activation process, it was transformed to potassium oxide by a dehydration reaction.

Potassium oxide reacts with carbon dioxide that is provided during physical activation to form K_2CO_3, which aids to form new pores and widen pores that were formed during chemical activation. So it was recognized that above 420 ^oC (melting point of KOH) the surface area of carbon activated by KOH is more than the area of carbon activated by K_2CO_3 [24].

When the IR reached to 1:1.5 the SSA increases at activation temperature of 600 ^oC, this may be due to lower potassium deposition on pores compared to the experiments of activation temperatures of 700 and 800 ^oC where the SSA decreased, this was probably due to excessive potassium hydroxide molecules decomposing into metal.

As a result, metal deposition on the already developed pores might have occurred and lead to a reduction of the surface area [25]. The relation between SSA, activation temperature, and impregnation ratio is shown in Fig. **2a**

Regarding the activation temperatures, it was perceived that as the temperature rises from 600 C^o to 700 ^oC with IR of the range 1:0.5- 1:1 the SSA increases with it.

These results showed that as the activation temperature increases, the structure tends to become micro porous.

That's due to that porosity is formed by KOH evaporation, therefore; as temperature increases, more KOH evaporates which leads to micro porosity enhancement, except for the result of the experiments with IR of 1:1.5, this is may be explained by the excessive concentration of KOH that led to the formation of wider or exploded pores which caused the declined SSA [26].

On the other hand, SSA decreased at 800 C^o, this is probably because high activating temperatures caused pore explosion that led to lower values of the specific surface area [27].

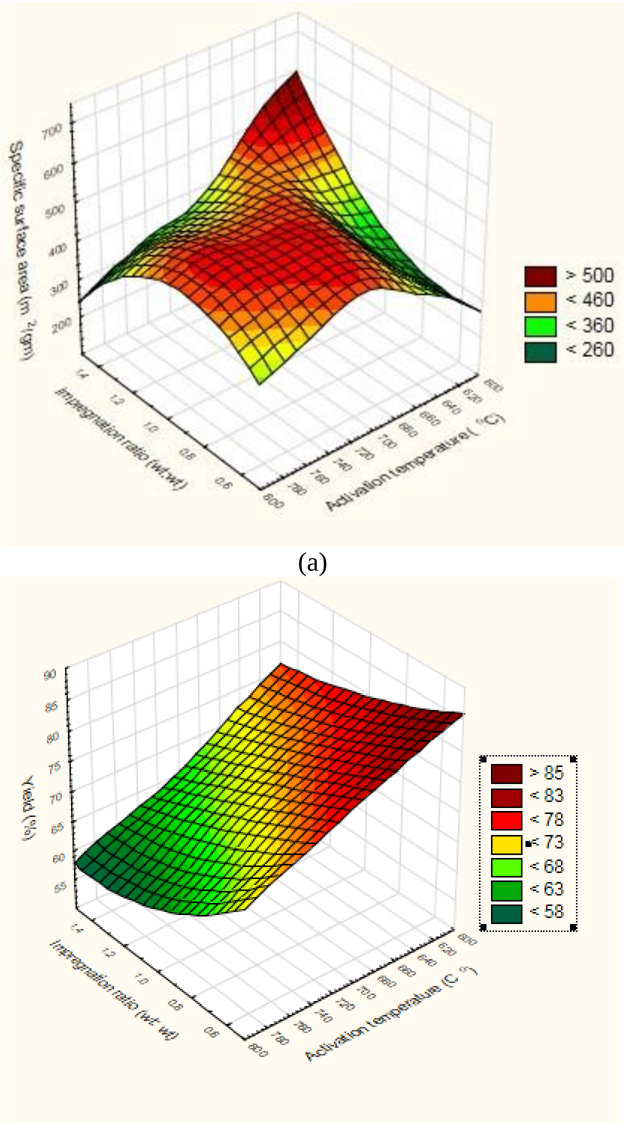

(a)

(b)

Fig. 2.

a) Effect of activation temperature and impregnation ratio on SSA

b) Effect of activation temperature and impregnation ratio on yield

In general, the CBAC yield was found to be inversely proportional to both temperatures of activation and IR. As temperature elevate more volatile components will be released due to intensified dehydration and elimination reaction that increases C-KOH and C-CO2 reaction rate, which causes lower [28]. As the IR value rises, KOH amount increases, which lead to oxidation process promotion causing the carbon atoms gasification reaction to become more dominant, therefore; more weight of carbon would be lost [24]. The relation between yield, activation temperature and impregnation ratio is shown in Fig. **2b**.

3.2. SEM and BET Analysis

Fig. **3** shows the SEM images of CB (a) and CBAC (b). It can be noticed that the CBAC surface has developed pores in which there is a good probability for chromium to be adsorbed. The BET surface area was 595.9 m^2/g.

Pore diameter in average was 3.46 nm, indicating that it was in the mesoporous region according to the International Union of Pure and Applied Chemistry (IUPAC). The pores are classified as micro pores (<2nm diameter), mesopores (2–50nm diameter) and macro pores (>50nmdiameter) [29].

The CBAC has a high surface area, which makes it more efficient for the removal of chromium. The high SSA of the CBAC was a result of the used technique of activation. The activation process involved chemical and physical activating agents which are KOH and CO_2 respectively. However, the developed pores during carbonization enhanced the surface area by diffusing more CO_2 and KOH molecules inside the pores, therefore; the reaction between KOH-carbon and CO_2-carbon promoted leading to more pores in the activated carbon.

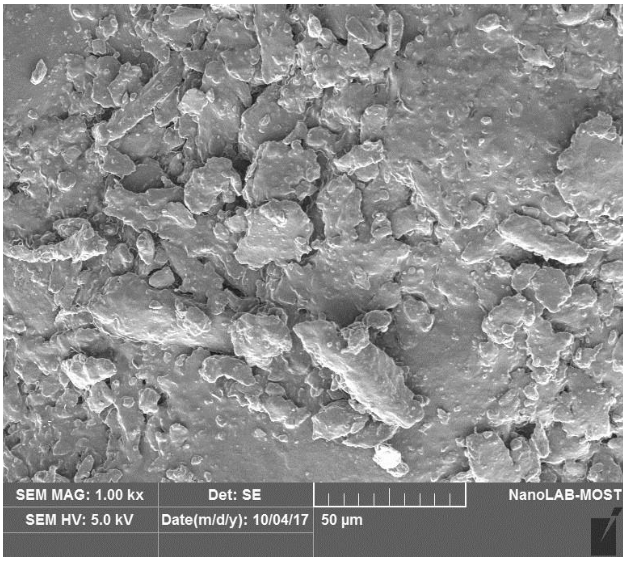

(a)

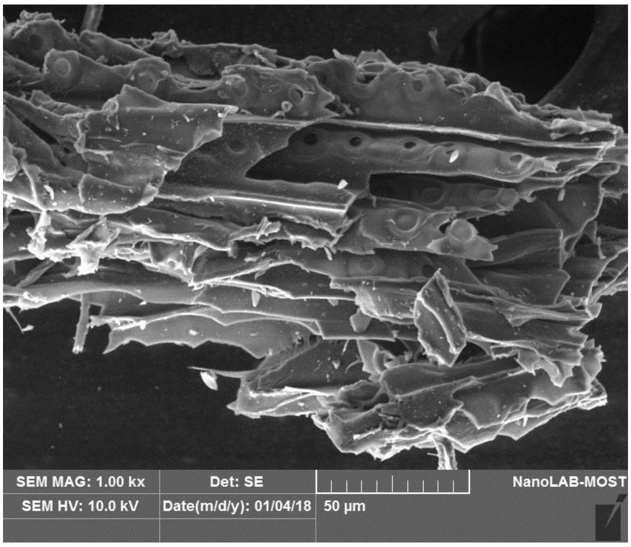

(b)

Fig. 3. SEM images, a) precursor b) CBAC (magnifications: 1000X)

3.3. Experimental Design and Empirical Model

The set of experiments that were designed by Taguchi method and their results are shown in Table **4**

Table 4. Batch adsorption experiments and their response

initial concentration (mg/L)	time (min)	Temperature (C)	pH	equilibrium concentration (mg/L)
10	30	20	2	6.51
10	120	30	5	7.4
10	210	40	8	3.41
10	300	50	11	5.275
20	30	30	8	15.285
20	120	20	11	11.63
20	210	50	2	6.418
20	300	40	5	5.66
30	30	40	11	23.52
30	120	50	8	12.14
30	210	20	5	6.487
30	300	30	2	3.35
50	30	50	5	35.89
50	120	40	2	13.13
50	210	30	11	18.6
50	300	20	8	9.22

In order to obtain the empirical model for the adsorption process the results from Taguchi experimental design was used. Y is the response variable, the obtained model with its four factors and their interaction is represented by:

$$Y = b_o + b_1X_1 + b_2X_2 + b_3X_3 + b_4X_4 + b_{12}X_1X_2 + b_{13}X_1X_3 + b_{14}X_1X_4 + b_{23}X_2X_3 + b_{24}X_2X_4 + b_{34}X_3X_4 + b_{11}X_1^2 + b_{22}X_2^2 + b_{33}X_3^2 + b_{44}X_4^2 \quad (6)$$

Where b_0, b_1, b_2, b_3 and b_4 are the linear coefficients, b_{12}, b_{13}, b_{14}, b_{23}, b_{24} and b_{34} are the second-order interaction terms, b_{11}, b_{22}, b_{33} and b_{44} are the quadratic terms of each factor. X_1, X_2, X_3 and X_4 are the coded terms of initial chromium concentration, time, temperature and pH, respectively.

The estimated values of the model coefficient, standard error of each model term and its p value are shown in Table **5**

Table 5. Model coefficients, standard error and terms p-values

	Estimate	Standard error	p- value
b0	7.506	1.869	0.00008
b1	0.443	0.047	0.00000
b2	-0.084	0.006	0.00000
b3	-0.016	0.815	0.00003
b4	-0.836	0.203	0.00005
b12	-0.001	0.000	0.00000
b13	-0.003	0.000	0.00000
b14	0.025	0.002	0.00000
b23	0.0001	0.000	0.265
b24	0.001	0.000	0.00000
b34	-0.005	0.002	0.044
b11	-0.001	0.000	0.035
b22	0.0002	0.000	0.00000
b33	0.0007	0.001	0.498
b44	0.063	0.11	0.00000

As it can be seen from table.4 that b_{23} and b_{33} have an insignificant effect on model accuracy, due to their p values, which are larger than 0.05.

3.4. Effects of Factors

a. Effect Of Contact Time And Cr(VI) Initial Concentration

The influence of adsorption time on chromium ions adsorbed by CBAC was investigated and presented in Fig. **4**. It was observed that the chromium ions removal efficiency by CBAC increased with the initial chromium ion concentration. The adsorption was fast at the initial stage because of the high driving force which induced the metal ions to transfer rapidly from the bulk solution to the surface of CBAC [17]. As time passed more active sited was occupied, this means less free active sites on the surface.

Alongside with the declined driving force that made the adsorption to take more time to reach equilibrium, because metal ions slowly diffused to the intra-particle pores of the adsorbent [30]. Thus, the adsorption rate is decreased.

It is also clear from Fig. **4** that removal efficiency improved as the initial concentration of Cr (II). Because of the increased driving force of the concentration gradient [31]. A similar trend of heavy metal adsorption, as a function of initial concentration, has also been reported previously [32], [33].

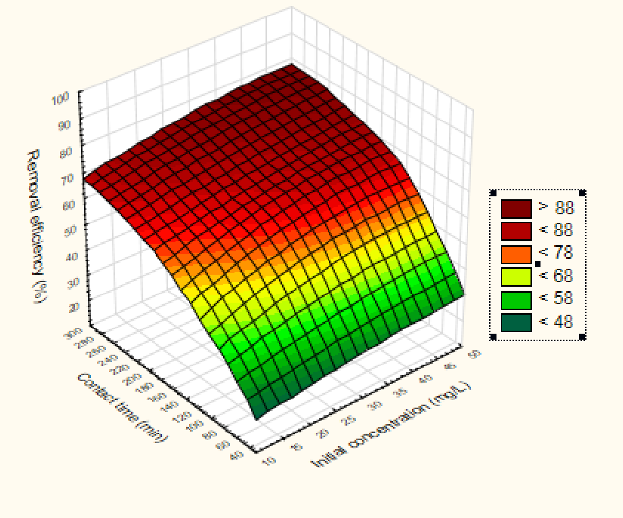

Fig. 4. Effect of contact time and initial concentration on removal efficiency

b. Effect Of ph And Temperature

The solution initial pH is the most significant factor to investigate the adsorption characteristic of an adsorbent because it affects not only surface charge of the adsorbent, but also the ionization degree and adsorbate speciation [34].

The effect of initial solution pH on chromium ion removal by CBAC is presented in Fig. **5**.

As the negative charge density on CBAC surface increases due to COOH ionization, the adsorbed chromium will rise rapidly [35]. At pH = 2, the efficiency on adsorption almost reached its maximum value.

As temperature rises, the solution viscosity will slightly decrease, which enhances the diffusion rate of chromium into the pores of CBAC [36]. In addition to that, the high temperatures will break internal bonds at the edges of the active sites [37], which aids the enhancement of adsorption efficiency of the CBAC. Fig. **5** illustrates the direct proportion between temperature and efficiency of adsorption.

As it can be seen from Fig. **5** that chromium adsorption on CBAC is an exothermic process.

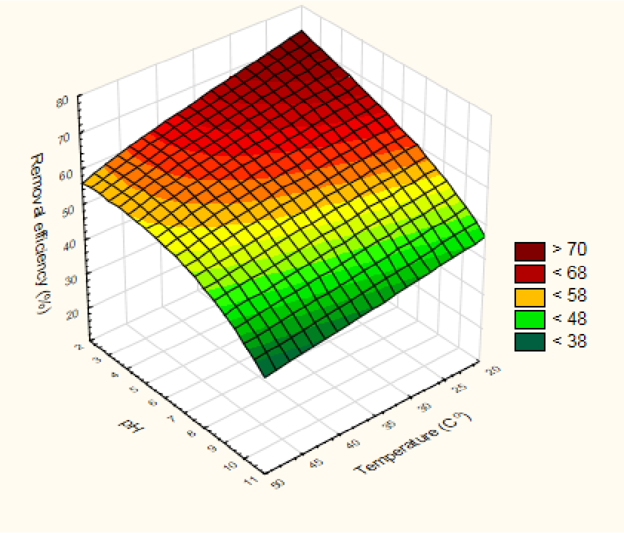

Fig. 5. The effect of initial pH and temperature on adsorption efficiency

3.5. Adsorption Isotherm Studies

The correlation between bulk solution concentration of sorbate and the amount of adsorbed heavy metal ions on the CBAC unit at equilibrium conditions is described functionally by the isotherms of adsorption. The adsorption isotherm was studied in order to understand the behavior of chromium ions in the solution – CBAC interphase,. Usually, adsorption isotherm analysis is conducted to find the fitter model to be used in equipment design purposes. Table.6 summarizes the capacities of adsorption for monolayer coverage as implied by the Langmuir model with the two isotherms constants and their correlation coefficients at 20, 30, 40 and 50 ˚C. As it can be observed that Freundlich model fitted adsorption data of Cr(VI) more adequately due to higher R^2 values at all the mentioned temperature range, where R^2 was more than 0.95. Fitting the Freundlich isotherm refers to the heterogeneous surface energies and high values of K_F indicate the high adsorption capacity of CBAC for Cr(VI) [38]. All 1/n values were larger than 1 which is an indication of the chemical nature of the process [39]. **Fig. 6** shows the plot of ln C_e versus ln q_e with temperature range of (20-50 ^oC). other studies had also confirmed the same results [40], [41].

Table 6. Values of Freundlich and Langmuir constants for Cr(VI) adsorption on CBAC

	Langmuir					
Temperature (C°)	K_L (L/mg)	q_m (mg/g)	R^2	KF (mg/g)	1/n	R^2
20	0.32	14.401	0.93	16.232	1.59	0.952
30	0.241	13.346	0.914	9.804	1.593	0.962
40	0.161	13.333	0.906	4.907	1.663	0.966
50	0.099	12.774	0.939	1.287	1.853	0.962

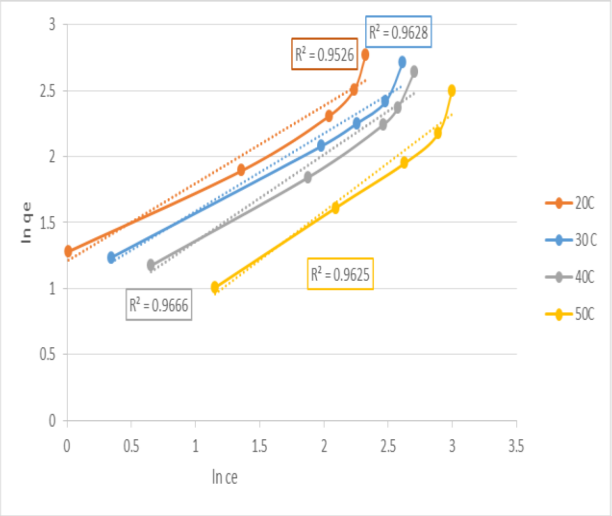

Fig. 6. Adsorption data fitted into Freundlich isotherm at temperature range of (20-50 C^o)

3.6. Kinetics Studies

To figure out the mechanism that controls the adsorption of chromium on CBAC, such as physical interactions and chemical reaction, pseudo-first-order and pseudo-second-order equations were utilized to model the kinetics of adsorption.

The comparison between the experimental and calculated concentration of equilibrium and correlation coefficients were used to evaluate kinetics equations fitting. As the difference between experimental equilibrium concentration (qe,exp) and calculated equilibrium concentration (qe,cal) get smaller and R2 goes to unity, the kinetic equation represents the adsorption more accurately.

The kinetics were studied at different initial concentration of chromium. Chromium adsorption obeyed pseudo-second order more clearly compared to pseudo-first order.

Pseudo-first order and pseudo-second order adsorption rate constants, calculated and experimental qe values for different initial concentration chromium are summarized in table 7. Other researches had confirmed the same results [37], [42] and [33].

Table 7. Comparison of the pseudo-first and pseudo-second order rate constants, and calculated and experimental qe values chromium adsorption on CBAC for various initial concentrations

		Pseudo-first order			Pseudo-second order		
Initial concentration (mg/L)	qe,exp (mg/g)	K_1 (1/min)	qe,cal (mg/g)	R^2	K_2 (g/mg min)	qe,cal (mg/g)	R^2
10	3.45	0.014	3.836	0.972	0.02	3.339	0.991
20	7.388	0.01	5.419	0.929	0.013	7.865	0.993
30	11.232	0.011	7.496	0.945	0.019	10.68	0.997
40	14.96	0.006	7.888	0.931	0.025	13.979	0.998
50	18.864	0.005	9.185	0.975	0.026	18.511	0.999

4- Conclusion

In this study, cow bones active carbon showed a promising prospect in chromium adsorption from aqueous solution over a wide range of conditions, the optimum removal efficiency was 94.32%. Highest SSA of CBAC was 595.9 m^2/g at the activation temperature of 600^oC and IR of 1:1.5.

Langmuir and Freundlich isotherm models were utilized to fit the data of equilibrium and the equilibrium data for CBAC were best represented by the Freundlich isotherm at different temperatures with R^2 values more than 0.95. The kinetics of adsorption followed the pseudo second-order kinetic model at various initial chromium concentrations; pseudo-second order kinetic model produced the highest R^2 values (more than 0.99). Due to the high range of removal efficiencies, CBAC can be used as a cost effective, inexpensive substitute to the commercial activated carbons.

References

[1] J. A. Alnajar, A. A. Kwaeri, R. H. Sayhood, and A. H. Slaymon, "Study the Feasibility of Alumina for the Adsorption of Metal Ions from Water," *Iraqi J. Chem. Pet. Eng.*, vol. 15, no. 3, pp. 37–50, 2014.

[2] A. H. Sulaymon, S. E. Ebrahim, T. J. Al Musawi, and S. M. Abdullah, "Removal of Lead , Cadmium , and Mercury Ions Using Biosorption," *Iraqi J. Chem. Pet. Eng.*, vol. 11, no. 2, pp. 1–13, 2010.

[3] W. Peng, H. Li, Y. Liu, and S. Song, "A review on heavy metal ions adsorption from water by graphene oxide and its composites," *J. Mol. Liq.*, vol. 230, pp. 496–504, 2017.

[4] A. A. El-Bayaa, N. A. Badawy, and E. A. Alkhalik, "Effect of ionic strength on the adsorption of copper and chromium ions by vermiculite pure clay mineral," *J. Hazard. Mater.*, vol. 170, no. 3, pp. 1204–1209, 2009.

[5] V. K. Gupta and I. Ali, "Removal of lead and chromium from wastewater using bagasse fly ash — a sugar industry waste," *J. ofColloid Interface Sci.*, vol. 271, pp. 321–328, 2004.

[6] F. An, R. Wu, M. Li, T. Hu, J. Gao, and Z. Yuan, "Removal of heavy metal ions by iminodiacetic acid functionalized D301 resin : Kinetics , isotherms and thermodynamics," *React. Funct. Polym.*, vol. 118, no. February, pp. 42–50, 2017.

[7] P. Kanagaraj, A. Nagendran, D. Rana, T. Matsuura, and S. Neelakandan, "Separation of macromolecular proteins and rejection of toxic heavy metal ions by PEI/cSMM blend UF membranes," *Int. J. Biol. Macromol.*, vol. 72, no. January 2015, pp. 223–229, 2014.

[8] F. Jos and I. Mart, "Transport of chromium (VI) through a Cyanex 921-supported liquid membrane from HCl solutions," *J. Chem. Technol. Biotechnol.*, vol. 1053, no. February 2003, pp. 1048–1053, 2003.

[9] P. Kanagaraj *et al.*, "Influence of N-phthaloyl chitosan on poly (ether imide) ultrafiltration membranes and its application in biomolecules and toxic heavy metal ion separation and their antifouling properties," *Appl. Surf. Sci.*, vol. 239, no. February 2015, pp. 165–173, 2014.

[10] G. Nemeth, L. Mlinarik, and A. Torok, "Adsorption and chemical precipitation of lead and zinc from contaminated solutions in porous rocks : Possible application in environmental protection," *J. African Earth Sci.*, vol. 122, no. October 2016, pp. 98–106, 2016.

[11] H. Sis and T. Uysal, "Removal of heavy metal ions from aqueous medium using Kuluncak (Malatya) vermiculites and effect of precipitation on removal," *Appl. Clay Sci.*, vol. 95, pp. 1–8, 2014.

[12] R. H. Salman, "Removal of Manganese Ions (Mn 2 +) from a Simulated Wastewater by Electrocoagulation / Electroflotation Technologies with Stainless Steel Mesh Electrodes : Process Optimization Based on Taguchi Approach," *Iraqi J. Chem. Pet. Eng.*, vol. 20, no. 1, pp. 39–48, 2019.

[13] S. Mahdavi, M. Jalali, and A. Afkhami, "Heavy metals removal from aqueous solutions using TiO2 , MgO , and Al2O3 nanoparticles," vol. 200, no. 3, pp. 448–470, 2016.

[14] M. A. Hashim, S. Mukhopadhyay, J. Narayan, and B. Sengupta, "Remediation technologies for heavy metal contaminated groundwater," *J. Environ. Manage.*, vol. 92, no. 10, pp. 2355–2388, 2011.

[15] J. Pallarés, A. González-Cencerrado, and I. Arauzo, "Production and characterization of activated carbon from barley straw by physical activation with carbon dioxide and steam," *Biomass and Bioenergy*, vol. 115, no. January, pp. 64–73, 2018.

[16] P. Chingombe, B. Saha, and R. J. Wakeman, "Surface modification and characterisation of a coal-based activated carbon," *Carbon N. Y.*, vol. 43, pp. 3132–3143, 2005.

[17] A. H. M. G. Hyder, S. A. Begum, and N. O. Egiebor, "Adsorption isotherm and kinetic studies of hexavalent chromium removal from aqueous solution onto bone char," *J. Environ. Chem. Eng.*, vol. 3, no. 2, pp. 1329–1336, 2014.

[18] J. C. Moreno-piraján, R. Gómez-cruz, V. S. García-cuello, and L. Giraldo, "Binary system Cu (II)/ Pb (II) adsorption on activated carbon obtained by pyrolysis of cow bone study," *J. Anal. Appl. Pyrolysis*, vol. 89, pp. 122–128, 2010.

[19] L. Massart and B. Vandeginste, *Chemometrics and qualimetrics in chemical engineering.* Newyork, NY: Princeton press, 1991.

[20] I. Langmuir, "The constitution and fundamental properties of solids and liquids.," *J. Am. Chem. Soc.*, vol. 182, pp. 2221–2295, 1916.

[21] H. Freundlich, "Capillary anf colloid chemistry. By Prof. H. Freundlich. Translated by H. Stafford Hatfield.," *J. Phys. Chem*, vol. 57, pp. 385–470, 1925.

[22] Y.-S. Ho, "Citation review of Lagergren kinetic rate equation on adsorption reactions," *Scientometrics*, vol. 59, no. 1, pp. 171–177, 2004.

[23] H. P. Boehm, "Some aspects of the surface chemistry of carbon blacks and other carbons," *Carbon N. Y.*, vol. 32, no. 5, pp. 759–769, 1994.

[24] Y. Sudaryanto, S. B. Hartono, W. Irawaty, H. Hindarso, and S. Ismadji, "High surface area activated carbon prepared from cassava peel by chemical activation," *Bioresour. Technol.*, vol. 97, no. March 2005, pp. 734–739, 2006.

[25] A. Borhan, M. F. Taha, and A. A. Hamzah, "Characterization of Activated Carbon from Wood Sawdust Prepared via Chemical Activation using Potassium Hydroxide," *Adv. Mater. Res.*, vol. 832, pp. 132–137, 2014.

[26] T. C. Chandra, M. M. Mirna, Y. Sudaryanto, and S. Ismadji, "Adsorption of basic dye onto activated carbon prepared from durian shell: Studies of adsorption equilibrium and kinetics," *Chem. Eng. J.*, vol. 127, no. 1–3, pp. 121–129, 2007.

[27] A. Nayak, B. Bhushan, V. Gupta, and P. Sharma, "Chemically activated carbon from lignocellulosic wastes for heavy metal waste-water remediation: effect of activation conditions.," *J. Colloid Interface Sci.*, vol. 493, pp. 228–240, 2017.

[28] M. Danish, R. Hashim, M. N. M. Ibrahim, and O. Sulaiman, "Optimized preparation for large surface area activated carbon from date (Phoenix dactylifera L.) stone biomass," *Biomass and Bioenergy*, vol. 61, no. 320, pp. 167–178, 2014.

[29] L. Niazi, A. Lashanizadegan, and H. Sharififard, "Chestnut oak shells activated carbon: Preparation, characterization and application for Cr (VI) removal from dilute aqueous solutions," *J. Clean. Prod.*, vol. 185, no. 6, pp. 554–561, 2018.

[30] I. Ullah, R. Nadeem, M. Iqbal, and Q. Manzoor, "Biosorption of chromium onto native and immobilized sugarcane bagasse waste biomass," *Ecol. Eng.*, vol. 60, pp. 99–107, 2013.

[31] E. Malkoc, Y. Nuhoglu, and M. Dundar, "Adsorption of chromium (VI) on pomace — An olive oil industry waste : Batch and column studies," *J. Hazard. Mater.*, vol. 138, pp. 142–151, 2006.

[32] E. Demirbas, M. Kobya, E. Senturk, and T. Ozkan, "Adsorption kinetics for the removal of chromium (VI) from aqueous solutions on the activated carbons prepared from agricultural wastes," *water SA*, vol. 30, no. 4, pp. 533–539, 2004.

[33] K. Li and X. Wang, "Bioresource technology adsorptive removal of Pb (II) by activated carbon prepared from Spartina alterniflora : Equilibrium , kinetics and thermodynamics," *Bioresour. Technol.*, vol. 100, no. 11, pp. 2810–2815, 2009.

[34] M. Imamoglu and O. Tekir, "Removal of copper (II) and lead (II) ions from aqueous solutions by adsorption on activated carbon from a new precursor hazelnut husks," *Desalination*, vol. 228, pp. 108–113, 2008.

[35] P. Miretzky, C. Munoz, and A. Carrillo-chavez, "Experimental binding of lead to a low cost on biosorbent: Nopal (Opuntia streptacantha)," *Bioresour. Technol.*, vol. 99, pp. 1211–1217, 2008.

[36] F. Boudrahem, "Batch sorption dynamics and equilibrium for the removal of lead ions from aqueous phase using activated carbon developed from coffee residue activated with zinc chloride," *J. Environ. Manage.*, vol. 90, pp. 3031–3039, 2009.

[37] J. Acharya, J. N. Sahu, B. K. Sahoo, C. R. Mohanty, and B. C. Meikap, "Removal of chromium (VI) from wastewater by activated carbon developed from Tamarind wood activated with zinc chloride," *Chem. Eng. J.*, vol. 150, pp. 25–39, 2009.

[38] M. B. Desta, "Batch Sorption Experiments : Langmuir and Freundlich Isotherm Studies for the Adsorption of Textile Metal Ions onto Teff Straw (Eragrostis tef) Agricultural Waste," *J. Thermodyn.*, vol. 20, pp. 375–380, 2013.

[39] N. Singh, A. Kumari, and C. Balomajumder, "Modeling studies on mono and binary component biosorption of phenol and cyanide from aqueous solution onto activated carbon derived from saw dust," *SAUDI J. Biol. Sci.*, vol. 25, no. 7, pp. 1454–1467, 2016.

[40] M. Jameel, "Study of Removal of Pb , Zn , Cu and Ni Ions from Iraqi factories wastewater using local porcelanite rocks," *Natl. J. Chem.*, vol. 39, pp. 445–454, 2010.

[41] M. Karnib, A. Kabbani, H. Holail, and Z. Olama, "Heavy metals removal using activated carbon , silica and silica activated carbon composite," *Energy Procedia*, vol. 50, pp. 113–120, 2014.

[42] Y. Li *et al.*, "Removal of lead from aqueous solution by activated carbon prepared from Enteromorpha prolifera by zinc chloride activation," *J. Hazard. Mater.*, vol. 183, no. 1–3, pp. 583–589, 2010.

امتزاز أيونات الكروم بواسطة كاربون منشط منتج من عظام البقر

الخلاصة

نتيجة للاستعمالات الواسعة للكروم في الصناعة، بالإضافة الى أن الكروم عنصر مسرطن، وجب البحث عن طريقه فعاله واقتصاديه لإزالته من المياه العادمة. في هذه الدراسة، تم استخدام عظام البقر، كماده اوليه رخيصة، لإنتاج الكاربون المنشط. تم تشخيص الكاربون المنتج بالمجهر الالكتروني للتحقق من شكله السطحي وتم استخدام ال(BET) لمعرفة مساحته السطحية. أفضل مساحه سطحيه تم الحصول عليها 595.9 متر مربع/ غم ب600 درجه سيلزيه كجرارة تفعيل و نسبة تصبيغ 1:1.5.

تم استخدام الكاربون المنتج من عظام البقر لامتزاز الكروم من المحاليل المائية. تم دراسة تأثير العوامل الأتية مع مدياتها: التركيز الاولي للكروم (10–50 ملغم/لتر)، وقت الامتزاز (30–300 دقيقه)، درجة الحرارة (20–50 درجه سيلزيه) والاس الهيدروجيني (2–11). تم تمثيل عملية الامتزاز رياضيا بواسطة معادله قياسيه تجريبيه. تم استخدام معادلة لانغماير وفريندليتش لقولبة عملية الامتزاز، حيث كانت العملية منطبقة أكثر على نموذج فريندليتش. استخدمت معادلة الدرجة الأولى والدرجة الثانية لدراسة حركيه الامتزاز، حيث كان الامتزاز متوافق أكثر مع معادلة الدرجة الثانية. أفضل كفاءه امتزاز كانت 94.32%.

الكلمات الدالة : امتزاز، كاربون منشط، عظام بقر، الكروم، تفعيل فيزيائي كيميائي.